

Accepted Manuscript

Full Length Article

Annealing temperature dependent reversible wettability switching of micro / nano structured ZnO superhydrophobic surfaces

Elmira Velayi, Reza Norouzbeigi

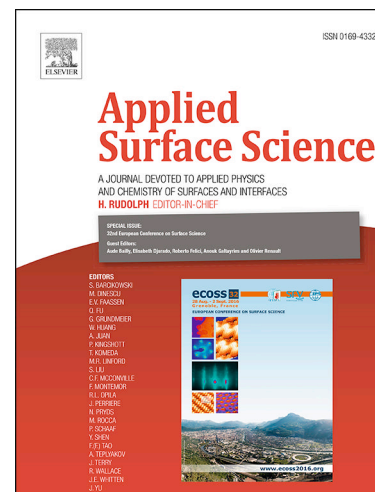
PII: S0169-4332(18)30348-9
DOI: <https://doi.org/10.1016/j.apsusc.2018.02.005>
Reference: APSUSC 38463

To appear in: *Applied Surface Science*

Received Date: 25 October 2017
Revised Date: 30 January 2018
Accepted Date: 1 February 2018

Please cite this article as: E. Velayi, R. Norouzbeigi, Annealing temperature dependent reversible wettability switching of micro / nano structured ZnO superhydrophobic surfaces, *Applied Surface Science* (2018), doi: <https://doi.org/10.1016/j.apsusc.2018.02.005>

This is a PDF file of an unedited manuscript that has been accepted for publication. As a service to our customers we are providing this early version of the manuscript. The manuscript will undergo copyediting, typesetting, and review of the resulting proof before it is published in its final form. Please note that during the production process errors may be discovered which could affect the content, and all legal disclaimers that apply to the journal pertain.



**Annealing temperature dependent reversible wettability switching of
micro /nano structured ZnO superhydrophobic surfaces**

Elmira Velayi¹, Reza Norouzbeigi^{1,*}

¹ Catalyst and Nanomaterials Laboratory, School of Chemical, Petroleum and Gas Engineering, Iran University of Science and Technology, P.B. 16765–163, Narmak, Tehran, Iran, e_velayi@chemeng.iust.ac.ir; norouzbeigi@iust.ac.ir

Abstract

Superhydrophobic ZnO surfaces with reversibly tunable wettability were fabricated on stainless steel meshes via a facile chemical bath deposition method just by regulating the micro/nano structured ZnO needles without using chemical post modifications. The obtained surfaces can be easily and reversibly switched between superhydrophobic and superhydrophilic/underwater superoleophobic characteristics by altering the annealing temperatures. As-prepared sample exhibited long-term superhydrophobic properties with a water contact angle (WCA) of $163.8^\circ \pm 1.8^\circ$ and contact angle hysteresis (CAH) of $1.1^\circ \pm 0.8^\circ$. The SEM, XRD, XPS and Raman analyses were employed to characterize the morphological features and surface chemistry of the prepared samples. SEM images showed the formation of ZnO micro/nanoneedles with a diameter of ~ 90 nm on the substrate. The superhydrophobic ZnO surface was switched to highly hydrophilic and underwater superoleophobic properties with an oil contact angle (OCA) of about 172.5° after being annealed at 400°C in air for 30 minutes and restored to superhydrophobic state again by altering the annealing temperature to 150°C . Mechanical durability of the ZnO superhydrophobic surface was tested by an abrasion test. Results confirmed that the prepared surface exhibited an excellent robustness after 20 abrasion cycles under the pressure of 4.7 KPa.

*Corresponding author: Tel./Fax: +98 2177240496, E-mail: norouzbeigi@iust.ac.ir

Keywords: micro/nano structured ZnO; chemical bath deposition; switchable wettability; superhydrophobic surface; underwater oleophobic

1.

2. Introduction

Surface wetting behavior is a determining property for application of solid materials in the smart microfluidic systems [1, 2], self-cleaning [3, 4], biomaterials [5-7], oil/water separation [8-10] and lab-on-cheap systems [11, 12] which are controlled by chemical composition and topographical structure [13-16]. Up to now various external stimuli such as UV irradiation [6, 17, 18], electric field [19, 20], thermal treatment [21, 22] and pH value alteration [23, 24] have been widely reported to change the wettability of surfaces. Among the reported stimulus-response pairs, the UV irradiation has been extensively investigated to convert the wetting properties of the photocatalyst metal oxides such as ZnO [25, 26], TiO₂ [27, 28], and SnO₂ [29] on different substrates. ZnO is one of the most important semiconductor metal oxides having some applications including self-cleaning [30, 31], anti-icing coatings [32] and optoelectronic devices like gas sensors [33, 34], light-emitting diodes [35, 36] and solar cells which exhibits photo-induced superhydrophilicity after at least 30 minutes UV irradiation and return to the hydrophobicity after long-term storage in a dark place (about several weeks or months) [37]. Li et al, fabricated hybrid ZnO/bamboo surfaces with reversible transition wettability characteristics [38]. They deposited well-aligned ZnO nano-sheet arrays on the bamboo surfaces via hydrothermal process following chemical treatment using octadecyltrichlorosilane. The surface wettability was switched between superhydrophilic and superhydrophobic situations via UV illumination for 12 h and dark storage for 10 days. Su and coworkers constructed superhydrophobic hierarchical bismuth nanostructures on zinc plates (WCA=164.8°) by the electroless deposition method and subsequent surface modification by stearic acid [39]. They also used the similar method to change the

wettability. Lian et al fabricated TiO₂ rough thin films on a titanium substrate [40]. The underwater oil wettability characteristics of rough surfaces were reversibly switched between superoleophobicity and oleophobicity by means of ethanol immersion and darkness storage. In the most of previous studies, the organic modifiers with poor thermal and chemical stabilities have been widely employed to fabricate superhydrophobic surfaces [3, 41-43]. On the other hand, the UV irradiation and long-term dark storage were widely applied to investigate the reversible wettability switching of inorganic semiconductor surfaces such as ZnO and TiO₂ because of their photo-induced superhydrophilicity properties [38, 44-46]. This technique is a time-consuming and expensive process. Therefore, it is necessary to consider the fabrication of inorganic superhydrophobic surfaces without post chemical treatment and enhancement of superwetting switching process speed.

In the recent years with increasing of industrial oily wastewater and accidental oil spills, the design and fabrication of surfaces with controllable wettability between superhydrophobicity/superoleophilicity (water contact angles larger than 150°) and superhydrophilicity/underwater superoleophobicity (oil contact angles larger than 150°) have attracted great interests in the field of oil/water separation [8-10, 17, 47].

In this study superhydrophobic ZnO nanostructured surfaces were developed on the stainless steel meshes by the facile and low-cost chemical bath deposition technique without post chemical modification. The reversibly switchable wettability of the prepared surfaces from superhydrophobicity/superoleophilicity to superhydrophilicity/underwater superoleophobicity was investigated by alteration of annealing temperature between 150° and 400° within a short time. The resulted surface can be used as a filter for on-demand oil/water separation which its wetting behavior can be reversibly switched between the superhydrophobic and superoleophobic characteristics based on the oil-water mixture, composition and density of the oil.

Materials and methods

2.1 Materials

Zinc (II) nitrate hexahydrate ($\text{Zn}(\text{NO}_3)_2 \cdot 6\text{H}_2\text{O}$), hexamethylenetetramine ($\text{C}_6\text{H}_{12}\text{N}_4$), ethanol ($\text{C}_2\text{H}_6\text{O}$), hexane (C_6H_{14}) and acetone ($\text{C}_3\text{H}_6\text{O}$) were purchased from Merck company. All reagents were used without further purification.

2.2 Sample preparation

Stainless steel meshes (type: 304) were cut into $2.5 \text{ cm} \times 2.5 \text{ cm}$, ultrasonically cleaned in distilled water, ethanol and acetone for 10 minutes, respectively. The cleaned substrates were etched with HNO_3 (4 M) for 20 min to remove oxide layers and then washed with distilled water again. The hierarchical zinc oxide films were fabricated on the substrate by a two-step synthesis process. First, the pretreated substrates were dipped in an ethanol solution containing zinc acetate dehydrate (20 mM) for 1 h. Afterward they were rinsed with ethanol and dried at 90°C for 1 h. Finally, the coated meshes were annealed in air at 400°C for 2 h led to nano ZnO seed layer formation on the substrates. In the next step, the as-prepared substrates were suspended vertically into the glass bottle involving an aqueous solution of zinc nitrate hexahydrate (0.025 M) and hexamethylenetetramine (0.0375 M). The glass bottle was heated in an oil bath at $90\text{-}100^\circ$ for 2 h. Samples were taken out of the solution and rinsed 2 times with ethanol and water, followed by drying in an oven at 150° for 6 h.

2.3 Reversible Switching wetting of ZnO micro/nano structured surface

The wettability transition of as-prepared samples from superhydrophobicity to superhydrophilicity state (underwater superoleophobicity) was performed by post-annealing treatment at 400°C for 30 min. The reverse wettability transition was obtained just by

decreasing the annealing temperature to 150°C during 6h. The proposed annealing process was conducted under ambient atmosphere (air) conditions.

2.4 Surface characterization

The crystallographic and chemical composition characteristics of the prepared surfaces were evaluated by X-ray diffractometer (X' Pert pro, model Panalytical, Netherlands) using nickel-filtered Cu K α radiation ($\lambda= 1.5418\text{\AA}$) and X-ray photoelectron spectrometer (XPS, SPECS XP Flex mode, Germany, equipped with a hemispherical PHOBIOS energy analyzer). Surface morphology of the samples was evaluated by scanning electron microscopy (SEM, Tescan, model VEGA2) operating at 30.0 kV. Raman spectra of samples were analyzed using a micro-Raman microscopy system (Lab Ram Horiba, High Spectra equipped with a HeNe laser ($\lambda= 532\text{ nm}$) at room temperature. Water contact angle (WCA), oil contact angle (OCA) and contact angle hysteresis (CAH) measurements in air and water mediums were performed using the sessile drop method [48], recorded with a digital optical microscope (DINOLITE, model AM-4113ZT, Taiwan). CAH values were evaluated via the oscillation method which is the difference between the advancing and receding static contact angles [48, 49]. For each surface, water and oil droplets were deposited with a volume of around 5 μl on the surface using a syringe pump (Zistrad, Iran) operated at 0.3 ml/min. This flow rate was also used for water injection and suction through a needle to measure the advancing and receding angles. The drop shape analysis plugin for the ImageJ software was applied to determine the contact angles. The WCA, CAH and OCA were measured at five different points of the samples and the average values are reported.

2.5 Mechanical durability test

The mechanical durability of the superhydrophobic ZnO sample was examined by measuring WCA after different abrasion cycles. In this test, the surface was moved back in two orthogonal directions (10 cm in each direction) on #400 sandpaper under the pressure of 4.7 KPa (300 g force).

3. Results and discussions

3.1 Switchable wettability and morphology of the superhydrophobic ZnO surfaces

Wetting behavior of solid surface plays an important role in many industrial processes. The common physical parameters for characterization of surface wettability behavior are static contact angle and contact angle hysteresis [48-50]. The water contact angle (WCA) and contact angle hysteresis (CAH) of as-prepared ZnO surface in the air were obtained $163.7^{\circ} \pm 1.8^{\circ}$ and $1.1^{\circ} \pm 0.8^{\circ}$, respectively. The heat treatment induced reversible wettability switches of ZnO surface between superhydrophobicity/superoleophilicity and superhydrophilicity/underwater superoleophobicity were evaluated by measuring water contact angle (WCA) and hexane contact angle (OCA) in air and water mediums, respectively. Results showed that the WCA and OCA of ZnO surface were changed respectively to $\sim 0^{\circ}$ and $172.5^{\circ} \pm 3$ after being treated at 400°C for 30 min in air atmosphere. The optical images of the water and hexane droplets on the as-prepared and annealed (400°C) samples are shown in Fig. 1. The WCA value of the obtained ZnO surface increased dramatically according to the annealing temperature reduction to 150°C and superhydrophobic properties were recovered during 6 h which is at least 10 times lower than those which have been reported by the other researchers [38, 51, 52]. For example, Li and coworkers used under ambient conditions dark place storage technique during a 10 day

period of time to reconvert the superhydrophobic state of a UV irradiated hybrid ZnO/bamboo surface [38]. The obtained results confirmed that the surface wetting behavior can be rapidly altered from superhydrophobicity to underwater superoleophobicity state by changing the annealing temperature from 150°C to 400° C and vice versa. To further investigate the wettability switching of the surfaces, annealing temperature alteration was repeated in four cycles as shown in Fig .2. It can be seen that more than 95% of the superhydrophobic and underwater superoleophobic properties were recovered successfully after the first annealing cycle (WCA= 161.7°, OCA= 160.5°). However, the fabricated ZnO surface wettability transition from superhydrophobicity to underwater superoleophobicity shows a completely reversible characteristic during the next cycles. Fig. 3 displays the changes of water droplet and under-water oil droplet contact angle hysteresis values vs. the annealing cycles. It can be seen that the water CAH values are in the range of 1-3° for the coated surfaces annealed at 150° C for 6 h. Upon further annealing treatment at 400° C for 30 min, the superhydrophobic ZnO surface exhibited under-water superoleophobic property with oil CAH results are lower than 3°. Additionally, the water CAH and oil CAH values maintained as low as ~3° after five repeated annealing cycles. It indicates excellent switchable wettability characteristics of the prepared ZnO surfaces.

Fig.1 Optical image of water and hexane droplets: (a) on the as-prepared ZnO surface, (b) after annealing at 400 °C.

Fig.2 Changes of WCA and underwater OCA values vs. annealing cycles.

Fig.3 Water droplet and underwater oil droplet CAH values vs. annealing cycles.

Theoretically, wetting behavior of a solid surface can be determined by its morphology and chemical composition [49, 53-56]. To acquire the information about the effect of annealing process on the ZnO-coated mesh microstructure, the scanning electron microscopy (SEM) analysis was applied. Fig.4 (a) indicates the bare stainless steel mesh with an average

wire diameter of 165 μm and pore size of 365 μm used as a substrate. The magnified SEM image of ZnO seed layer in Fig. 4(b) confirms a uniform distribution of ZnO nano seeds with particle sizes of 85 nm to 95 nm on the substrate. These nanoparticles can be served as nucleation sites for subsequent growth of nanostructured ZnO films [57, 58]. Figs. 4 (c) and (d) show the SEM images of superhydrophobic ZnO coating on the substrate. It can be seen that the hierarchical ZnO micro/nano structured films composed of ZnO nano needles with a diameter of ~ 90 nm and the length of approximately several micrometers are formed on the stainless steel mesh. In the most of studies low surface free energy materials such as fluoropolymers, fatty acids and silane coupling agents are used to modify the roughened ZnO surfaces for obtaining the superhydrophobicity state [59-63]. Evaluation of the obtained WCA values reveals that the superhydrophobicity can be obtained just by regulating the micro/nano structured needles of ZnO without using any further chemical modifier [55, 64]. The WCA values of the surface didn't change after six months exposure to the ambient air proving an excellent stability and time-independent wetting property.

The Wenzel and Cassie-Baxter theories are two main models that describe the wettability of micro/nano roughened surfaces with high static water contact angles [14, 48, 50]. However, in the case of water adhesion, these two theories present and assume different behaviors [49, 65]. In the Cassie-Baxter state, air entrapment between the liquid and solid surface leads to a significant reduction of water adhesion. Thus the CAH values decrease dramatically and the droplets can easily roll over the surface. In the Wenzel state, the water droplets can fill the rough surface which results in high water adhesion to the surface and consequently CAH values increase. In the present case regarding the low CAH value ($< 10^\circ$) and high WCA ($> 150^\circ$), the Cassie-Baxter state can exhibit the wetting properties of hierarchical micro/nano structured ZnO surfaces, as shown in Eq.1.

$$\cos\theta^* = f_1\cos\theta - f_2 \quad (f_1 + f_2 = 1) \quad (1)$$

Where the terms of f_1 , f_2 , θ and θ^* represent the fraction of the solid-liquid interface, the fraction of the solid-air interface, the smooth surface apparent contact angle and the rough surface contact angle, respectively.

SEM images of the superhydrophilic/superoleophobic ZnO surface are displayed in Figs. 4 (e) and (f). It can be clearly observed that there is no obvious change in the morphology and microstructure of the surface after annealing process at 400 °C. So, the alteration of annealing temperature doesn't affect the morphology of ZnO coating.

Fig. 4 SEM images of the 304-stainless-steel mesh surface :(a) bare substrate, (b) with a seed layer of ZnO, (c) and (d) as- prepared ZnO surface, (e) and (f) after annealing at 400° C.

3.2 XRD analysis

The XRD analysis was conducted to examine the crystal structure of ZnO surfaces with switchable wettability. Figs. 5a and 5b show the XRD patterns of ZnO surfaces (the as-prepared sample and sample annealed at 400 °C). It was found that both XRD patterns present similar characteristic peaks at 31.8°, 34.3°, 36.2°, 47.5°, 56.7°, 62.7° and 66.2°, 67.8°, 68.9° which are related to (1 0 0), (0 0 2), (1 0 1), (1 0 2), (1 1 0), (1 0 3), (2 0 0), (1 1 2), and (2 0 1) planes of ZnO, respectively. These diffraction peaks agree with hexagonal wurtzite structure according to JCPDS card no. 00-047-0956 [66]. Three characteristic peaks observed at 43.5°, 50.7° and 74.6° can be attributed to the cubic structure of 304-stainless steel mesh (JCPDS card no.00-033-0397) [67]. As it is evident from this figure, both samples exhibited preferential orientation along (101) crystal plane. In addition, the sharp peaks appeared in the XRD pattern related to the sample annealed at 400 °C indicate a good crystallinity compared to as-prepared

sample.

Fig. 5 XRD pattern of samples: (a) as-prepared, (b) annealed sample at 400° C.

3.3 Chemical composition analysis

XPS and Raman analyses were applied to investigate the influence of the annealing process on the chemical composition of micro/nano ZnO surface. As no obvious morphological changes were observed, the wettability variation may be related to the surface chemistry changes of the ZnO coatings. ZnO is a well-known semiconductor which shows photo-induced hydrophilicity under UV illumination [68-70]. It leads to the surface wettability change from the originally hydrophilic state to the superhydrophilicity (WCA ~ 0°). Therefore, the intrinsic hydrophilic characteristic of the ZnO surfaces may be assigned to the presence of hydroxyl groups and the oxygen defects [46, 51, 71]. Hu et al. reported that the interaction energy per area between water molecules and a hydrated ZnO surface with oxygen vacancies is much higher oxygen vacancies presence. The highly hydrophilic ZnO coatings were obtained in the presence of oxygen vacancies with water contact angle of ~ 21°[72]. In general, the oxygen vacancies on the ZnO surface change the homogeneity of the electron density of the surface and make it easier to become wet by the polar molecules such as water [52, 69, 73]. Fig. 6 shows the X-ray photoelectron spectra of the as-prepared and annealed samples. Strong peaks of zinc, oxygen and a weak signal of carbon were detected as shown in three survey spectra. The detected weak carbon peak is assigned to carbon contamination in the ambient air which was adsorbed on the samples [18, 74]. Figs. 7 (a) and (b) display the O1s spectra for ZnO samples with switchable wettability. The O1s spectra of as-prepared and annealed samples were deconvoluted into three peaks positioned at 530.5 ± 0.5 eV, 531.2 ± 0.2 eV and 532.4 ± 0.1 eV using Gaussian fitting analysis. The first peak can be

ascribed to O^{2-} ions in the Zn-O bond [75-79]. The second one is related to surface hydroxyl groups and oxygen vacancies. The appeared peak at 532 eV is attributed to the oxygen bonds with carbon (C-O, C=O) and H_2O . As it is evident from the fig. 7, amounts of oxygen in hydroxyl groups increased by the annealing process at 400 °C. This process increased hydroxyl group content of ZnO surface from 33.8% to 45.1%. High-temperature annealing process creates oxygen defects on ZnO surface which possess a further high capability to bind the hydroxyl groups[69]. Qui et al. confirmed that the increasing of post-annealing temperatures up to 300°C leads to desorption of oxygen in the zinc oxide lattice and formation of new surface defects on the sample surface [80]. Generally, high-temperature annealing of ZnO surfaces generates electron-hole pairs [38, 81, 82]. The electron-hole pairs move to the surface and react with the lattice metal ions (Zn^{2+}) and the lattice oxygen to form the defective sites (Zn^+) and oxygen vacancies, respectively. In this condition, -OH groups and oxygen molecules compete to be adsorbed on these sites while hydroxyl group adsorption is more favorable kinetically than those oxygen molecules [69, 70, 83, 84]. In recent years, several studies have been conducted to identify the effect of oxygen vacancies on the wettability of ZnO surface. In this way, Mrabet et al. explained the wetting properties of ZnO surface based on the Fowkes's approach (considering Lewis acid-base interactions) [85, 86]. The presence of oxygen vacancies improves the acid characteristic of the surface and promotes interactions with H_2O which is considered as a Lewis base in this case. Kinetically, rate of the present adsorbing electrophilic sites occupation by water molecules and accordingly formation of the hydroxyl groups is high. The high surface energy of the hydroxyl groups results in hydrophilic surface properties. Underwater, the water molecules are effectively trapped in the hierarchical micro/nano dual scale structure of these surfaces [87]. These phenomena lead to water cohesion between oil and the solid surface which enables the oil droplets to roll off. Therefore, the presence of oxygen-deficient sites is another

influential factor which changes the wettability characteristic to hydrophilic property [72, 86]. The hydroxyl groups adsorbed on the defect sites are thermodynamically unstable. In fact, geometric and electrical structures of the ZnO surfaces are distorted by adsorption of the hydroxyl groups [51, 69]. Considering the high free energy level, this situation is considered as a very unstable state compared to the native (grounded) hydrophobic ZnO surface [38, 81]. Reasonably, zinc oxide surface exposure to the ambient atmosphere leads to break of the adsorption equilibrium and according to the thermodynamic point of view; it promotes the preferred adsorption of the oxygen molecules on the surface to suppress the instability [88, 89]. In this way, active sites of the ZnO structures return to their original stable state. Heat treatment of the hydrophilic surface at 150 °C can accelerate the reduction of the oxygen vacancy of the sample surface and eliminate the hydroxyl groups [69]. Reasonably, the surface returned to the superhydrophobicity. Thus the variation of annealing temperature from 150°C to 400°C resulted in reversible alteration of wettability between superhydrophobicity and superhydrophilicity situations.

Fig. 6 XPS wide survey spectra of samples: (a) as-prepared, (b) annealed at 400° C.

Fig.7 XPS O 1s spectra of samples: (a) as-prepared, (b) annealed at 400° C.

Raman spectroscopy analysis was used to evaluate the effect of ZnO surface composition. Figs. 8 (a), (b) and (c) present the Raman spectra of as-prepared and annealed samples at different temperatures, 400°C and 150°C, respectively. The peaks marked at 95, 323, 376, 434, 580 and 1140 cm^{-1} are obviously assigned to ZnO [91, 92]. Comparison between the results confirms that a wide peak centered at 580 cm^{-1} is observed with the increase of annealing temperature up to 400° C. This peak becomes weaker and it disappears completely upon the next heat treatment step at 150°C (Fig 7 (c)). According to the literature data,

Raman shift positioned in the region of $560\text{-}580\text{ cm}^{-1}$ is related to the oxygen vacancy defect[93]. These results confirm that the oxygen vacancy of the sample (b) is more than that of the sample (a) and the sample (c). In other words, the absence of oxygen vacancy defects causes the obtained superhydrophobic properties of micro/nano structured ZnO surfaces which are in agreement with XPS results.

Fig. 8 Raman spectra of samples: (a) as-prepared, (b) after annealing at 400°C , (c) after annealing at 150°C .

3.4 Mechanical durability of superhydrophobic as-prepared sample

The mechanical durability of superhydrophobic surfaces is one of the most important factors to study the applicability of surfaces in the industry. The simple and common method to test the mechanical durability of superhydrophobic surfaces is the abrasion test. In this method the WCA and CAH are usually measured after each abrasion cycle to evaluate the mechanical resistance of the superhydrophobic surfaces [94-97]. The measured WCA and CAH values resulted from different abrasion cycles are shown in Fig.9. It can be seen that the variation of WCA values is in the range of 163.8° and 141° which shows no significant changes after 20 abrasion cycles. In addition, the CAH alteration is almost low in the range of 1.17° to 3.95° which confirms that the surface maintained its superhydrophobic wetting characteristics. The SEM images of the sample after mechanical abrasion tests are illustrated in Fig.10. Although some parts of the superhydrophobic coating were destroyed, the hierarchical micro/nano structures were preserved. This dual structure is very critical for retaining the surface superhydrophobic properties according to the Cassie-Baxter state. The obtained results reveal a better mechanical durability comparison with some previous literature reports [98-101]. The mechanical robustness of hierarchically structured superhydrophobic

silicon surface has been evaluated using a similar abrasion test[101]. Results showed that the CAH increased largely from $\sim 2^\circ$ to 13° and the superhydrophobicity character disappeared for abrasion length of 25cm (in one direction) under pressure of 3.45 KPa. Liu et al. constructed a superhydrophobic Cu surface with dual-scale roughness[100]. The abrasion resistance of the surface was examined by applying a normal pressure (~ 5 KPa) using cotton fabric. The WCA values decreased noticeably from 170° to 153° under a similar length of abrasion. The stability of a superhydrophobic steel surface has been studied by Latthe et al. using SiC sandpapers (600 grit) as abrasion surface[98]. Related report confirmed that the CAH values were significantly increased and the non-sticky superhydrophobic behavior of the prepared surface was irreversibly changed to sticky state under loading of a 500 g weight and abrasion length of ~ 100 cm.

Fig. 9 Variations in WCA values related to the as-prepared superhydrophobic sample after abrasion cycles.

Fig.10 SEM images of superhydrophobic surface after 20 cycles of abrasion test. (a) Low magnification (100x) and (b) high magnification (30000x).

4. Conclusion

In summary, a smart superhydrophobic ZnO surface with switchable wettability has been developed on the basis of controlling surface chemical composition. The as-prepared ZnO coated stainless steel mesh exhibits the excellent superhydrophobic properties with the WCA of about $163.8^\circ \pm 1.8^\circ$ and CAH of $1.1^\circ \pm 0.8^\circ$. Resulted surface became underwater oleophobic after annealing process at 400°C for 30 minutes. The surface wettability recovered to the initial superhydrophobic state via the annealing condition shift to 150°C for 6 h. XPS and Raman analyses confirmed that the amounts of the hydroxyl group and oxygen-deficient sites are responsible for the

switchable wettability. Moreover, the obtained ZnO surface showed an excellent abrasion resistance after 20 cycles upon the pressure of 4.7 KPa.

References

- [1] M. Elsharkawy, T.M. Schutzius, C.M. Megaridis, Inkjet patterned superhydrophobic paper for open-air surface microfluidic devices, *Lab on a Chip*, 14 (2014) 1168-1175.
- [2] O.I. Vinogradova, A.L. Dubov, Superhydrophobic Textures for Microfluidics, *Mendeleev Commun.* 22 (2012) 229-236.
- [3] H. Li, S. Yu, A robust superhydrophobic surface and origins of its self-cleaning properties, *Appl. Surf. Sci.* 420 (2017) 336-345.
- [4] S.S. Moosavi, R. Norouzbeigi, E. Velayi, Fabrication of flower-like micro/nano dual scale structured copper oxide surfaces: Optimization of self-cleaning properties via Taguchi design, *Appl. Surf. Sci.* 422 (2017) 787-797.
- [5] C.-R. Hsiao, C.-W. Lin, C.-M. Chou, C.-J. Chung, J.-L. He, Surface modification of blood-contacting biomaterials by plasma-polymerized superhydrophobic films using hexamethyldisiloxane and tetrafluoromethane as precursors, *Appl. Surf. Sci.* 346 (2015) 50-56.
- [6] Y. Su, C. Luo, Z. Zhang, H. Hermawan, D. Zhu, J. Huang, Y. Liang, G. Li, L. Ren, Bioinspired surface functionalization of metallic biomaterials, *J. Mech. Behav. Biomed. Mater.* 77 (2018) 90-105.
- [7] Z. Zang, X. Tang, Enhanced fluorescence imaging performance of hydrophobic colloidal ZnO nanoparticles by a facile method, *J. Alloy. Comp.* 619 (2015) 98-101.
- [8] Y. Song, Y. Liu, B. Zhan, C. Kaya, T. Stegmaier, Z. Han, L. Ren, Fabrication of Bioinspired Structured Superhydrophobic and Superoleophilic Copper Mesh for Efficient oil-water Separation, *J. Bionic Eng.* 14 (2017) 497-505.
- [9] W. Yang, J. Li, P. Zhou, L. Zhu, H. Tang, Superhydrophobic copper coating: Switchable wettability, on-demand oil-water separation, and antifouling, *Chem. Eng. J.* 327 (2017) 849-854.
- [10] H. Zhu, Z. Guo, Understanding the Separations of Oil/Water Mixtures from Immiscible to Emulsions on Super-wettable Surfaces, *J. Bionic Eng.* 13 (2016) 1-29.
- [11] E. Gogolides, K. Ellinas, A. Tserepi, Hierarchical micro and nano structured, hydrophilic, superhydrophobic and superoleophobic surfaces incorporated in microfluidics, microarrays and lab on chip microsystems, *Microelectron. Eng.* 132 (2015) 135-155.
- [12] G. Londe, A. Chunder, A. Wesser, L. Zhai, H.J. Cho, Microfluidic valves based on superhydrophobic nanostructures and switchable thermosensitive surface for lab-on-a-chip (LOC) systems, *Sens. Actuators B. Chem.* 132 (2008) 431-438.
- [13] X.J. Feng, L. Jiang, Design and Creation of Superwetting/Antiwetting Surface, *Adv. Mater.* 18 (2006) 3063-3078.
- [14] G. Wang, Z. Guo, W. Liu, Interfacial Effects of Superhydrophobic Plant Surfaces: A Review, *J. Bionic Eng.* 11 (2014) 325-345.
- [15] R.J. Crawford, E.P. Ivanova, Chapter Three - The Design of Superhydrophobic Surfaces, in: *Superhydrophobic Surfaces*, Elsevier, Amsterdam, 2015, pp. 27-49.
- [16] T.A. Otitoju, A.L. Ahmad, B.S. Ooi, Superhydrophilic (superwetting) surfaces: A review on fabrication and application, *J. Ind. Eng. Chem.* 47 (2017) 19-40.
- [17] L. Yan, J. Li, W. Li, F. Zha, H. Feng, D. Hu, A photo-induced ZnO coated mesh for on-demand oil/water separation based on switchable wettability, *Mater. Lett.* 163 (2016) 247-249.
- [18] B. Zhang, S. Lu, W. Xu, Y. Cheng, Controllable wettability and morphology of electrodeposited surfaces on zinc substrates, *Appl. Surf. Sci.* 360 (2016) 904-914.
- [19] L. Xu, W. Chen, A. Mulchandani, Y. Yan, Reversible Conversion of Conducting Polymer Films from Superhydrophobic to Superhydrophilic, *Angewandte Chemie International Edition*, 44 (2005) 6009-6012.

- [20] L. Xu, Q. Ye, X. Lu, Q. Lu, Electro-Responsively Reversible Transition of Polythiophene Films from Superhydrophobicity to Superhydrophilicity, *ACS Appl. Mater. Interfaces*. 6 (2014) 14736-14743.
- [21] Z. Wang, L. Zhu, W. Li, H. Liu, Rapid Reversible Superhydrophobicity-to-Superhydrophilicity Transition on Alternating Current Etched Brass, *ACS Appl. Mater. Interface*. 5 (2013) 4808-4814.
- [22] Y. Shi, W. Yang, J. Bai, X. Feng, Y. Wang, Fabrication of flower-like copper film with reversible superhydrophobicity–superhydrophilicity and anticorrosion properties, *Surf. Coat. Technol.* 253 (2014) 148-153.
- [23] M. Cheng, Q. Liu, G. Ju, Y. Zhang, L. Jiang, F. Shi, Bell-Shaped Superhydrophilic–Superhydrophobic–Superhydrophilic Double Transformation on a pH-Responsive Smart Surface, *Adv. Mater.* 26 (2014) 306-310.
- [24] B. Wang, Z. Guo, W. Liu, pH-responsive smart fabrics with controllable wettability indifferent surroundings, *RSC Adv.* 4 (2014) 14684-14690.
- [25] X. Zhu, Z. Zhang, X. Men, J. Yang, X. Xu, Fabrication of an intelligent superhydrophobic surface based on ZnO nanorod arrays with switchable adhesion property, *Appl. Surf. Sci.* 256 (2010) 7619-7622.
- [26] J. Li, Z. Jing, Y. Yang, F. Zha, L. Yan, Z. Lei, Reversible low adhesive to high adhesive superhydrophobicity transition on ZnO nanoparticle surfaces, *Appl. Surf. Sci.* 289 (2014) 1-5.
- [27] W. Li, T. Guo, T. Meng, Y. Huang, X. Li, W. Yan, S. Wang, X. Li, Enhanced reversible wettability conversion of micro-nano hierarchical TiO₂/SiO₂ composite films under UV irradiation, *Appl. Surf. Sci.* 283 (2013) 12-18.
- [28] S.-F. Wang, T.-H. Kao, C.-C. Cheng, C.-J. Chang, J.-K. Chen, Reversible manipulation of the adhesive forces of TiO₂/polybenzoxazine nanoassembled coatings through UV irradiation and thermal treatment, *Appl. Surf. Sci.* 357 (2015) 1634-1646.
- [29] W. Zhu, X. Feng, L. Feng, L. Jiang, UV-Manipulated wettability between superhydrophobicity and superhydrophilicity on a transparent and conductive SnO₂ nanorod film, *Chem. Commun.* (2006) 2753-2755.
- [30] V.H. Tran Thi, B.-K. Lee, Development of multifunctional self-cleaning and UV blocking cotton fabric with modification of photoactive ZnO coating via microwave method, *J. Photochem. Photobiol A Chem.* 338 (2017) 13-22.
- [31] T.S.G. Raja, K. Jeyasubramanian, Tuning the superhydrophobicity of magnesium stearate decorated ZnO porous structures for self-cleaning urinary coatings, *Appl. Surf. Sci.* 423 (2017) 293-304.
- [32] M. Zhang, S. Zhan, Z. He, J. Wang, L. Wang, Y. Zheng, J. Liu, Robust electrical uni-directional deicing surface with liquid (Ga₉₀In₁₀) and ZnO nano-petal composite coatings, *Mater. Des.* 126 (2017) 291-296.
- [33] L. Zhu, W. Zeng, Room-temperature gas sensing of ZnO-based gas sensor: A review, *Sens. Actuators, A*. 267 (2017) 242-261.
- [34] V. Galstyan, E. Comini, C. Baratto, G. Faglia, G. Sberveglieri, Nanostructured ZnO chemical gas sensors, *Ceram. Int.* 41 (2015) 14239-14244.
- [35] M.N. Rezaie, N. Manavizadeh, E.M.N. Abadi, E. Nadimi, F.A. Boroumand, Comparison study of transparent RF-sputtered ITO/AZO and ITO/ZnO bilayers for near UV-OLED applications, *Appl. Surf. Sci.* 392 (2017) 549-556.
- [36] Z. Zang, X. Zeng, J. Du, M. Wang, X. Tang, Femtosecond laser direct writing of microholes on roughened ZnO for output power enhancement of InGaN light-emitting diodes, *Opt. Lett.* 41 (2016) 3463-3466.
- [37] Z. Zang, A. Nakamura, J. Temmyo, Single cuprous oxide films synthesized by radical oxidation at low temperature for PV application, *Opt. Express*. 21 (2013) 11448-11456.
- [38] J. Li, Q. Sun, S. Han, J. Wang, Z. Wang, C. Jin, Reversibly light-switchable wettability between superhydrophobicity and superhydrophilicity of hybrid ZnO/bamboo surfaces via alternation of UV irradiation and dark storage, *Prog. Org. Coat.* 87 (2015) 155-160.
- [39] C. Su, Z. Lu, H. Zhao, H. Yang, R. Chen, Photoinduced switchable wettability of bismuth coating with hierarchical dendritic structure between superhydrophobicity and superhydrophilicity, *Appl. Surf. Sci.* 353 (2015) 735-743.

- [40] Z. Lian, J. Xu, Z. Wang, Z. Weng, Z. Xu, H. Yu, Reversibly switchable wettability between underwater superoleophobicity and oleophobicity of titanium surface via ethanol immersion and dark storage, *Appl. Surf. Sci.* 390 (2016) 244-247.
- [41] E.V. Bryuzgin, V.V. Klimov, S.A. Repin, A.V. Navrotskiy, I.A. Novakov, Aluminum surface modification with fluoroalkyl methacrylate-based copolymers to attain superhydrophobic properties, *Appl. Surf. Sci.* 419 (2017) 454-459.
- [42] L. Feng, Y. Zhu, J. Wang, X. Shi, One-step hydrothermal process to fabricate superhydrophobic surface on magnesium alloy with enhanced corrosion resistance and self-cleaning performance, *Appl. Surf. Sci.*, 422 (2017) 566-573.
- [43] B. Wang, Y. Hua, Y. Ye, R. Chen, Z. Li, Transparent superhydrophobic solar glass prepared by fabricating groove-shaped arrays on the surface, *Appl. Surf. Sci.*, 426 (2017) 957-964.
- [44] G. Kenanakis, E. Stratakis, K. Vlachou, D. Vernardou, E. Koudoumas, N. Katsarakis, Light-induced reversible hydrophilicity of ZnO structures grown by aqueous chemical growth, *Appl. Surf. Sci.* 254 (2008) 5695-5699.
- [45] S. Banerjee, D.D. Dionysiou, S.C. Pillai, Self-cleaning applications of TiO₂ by photo-induced hydrophilicity and photocatalysis, *Appl. Catal. B Environ.* 176-177 (2015) 396-428.
- [46] H. Ennaceri, L. Wang, D. Erfurt, W. Riedel, G. Mangalgi, A. Khaldoun, A. El Kenz, A. Benyoussef, A. Ennaoui, Water-resistant surfaces using zinc oxide structured nanorod arrays with switchable wetting property, *Surf. Coat. Technol.* 299 (2016) 169-176.
- [47] J. Li, P. Guan, Y. Zhang, B. Xiang, X. Tang, H. She, A diatomite coated mesh with switchable wettability for on-demand oil/water separation and methylene blue adsorption, *Sep. Purif. Technol.* 174 (2017) 275-281.
- [48] V. Senez, V. Thomy, R. Dufour, Characterization Techniques for Super Non-Wetting Surfaces, in: *Nanotechnologies for Synthetic Super Non-Wetting Surfaces*, John Wiley & Sons, Inc., 2014, pp. 109-147.
- [49] A. Milionis, E. Loth, I.S. Bayer, Recent advances in the mechanical durability of superhydrophobic materials, *J. Adv. Colloid Interface Sci.* 229 (2016) 57-79.
- [50] V. Mortazavi, M.M. Khonsari, On the degradation of superhydrophobic surfaces: A review, *Wear*, 372 (2017) 145-157.
- [51] X. Feng, L. Feng, M. Jin, J. Zhai, L. Jiang, D. Zhu, Reversible Super-hydrophobicity to Super-hydrophilicity Transition of Aligned ZnO Nanorod Films, *J. Am. Chem. Soc.* 126 (2004) 62-63.
- [52] S.N. Das, J.H. Choi, J.P. Kar, J.M. Myoung, Tunable and reversible surface wettability transition of vertically aligned ZnO nanorod arrays, *Appl. Surf. Sci.* 255 (2009) 7319-7322.
- [53] E. Celia, T. Darmanin, E. Taffin de Givenchy, S. Amigoni, F. Guittard, Recent advances in designing superhydrophobic surfaces, *J. Adv. Colloid Interface Sci.* 402 (2013) 1-18.
- [54] X. Gao, Z. Guo, Biomimetic Superhydrophobic Surfaces with Transition Metals and Their Oxides: A Review, *J. Bionic Eng.* 14 (2017) 401-439.
- [55] E. Velayi, R. Norouzbeigi, Robust superhydrophobic needle-like nanostructured ZnO surfaces prepared without post chemical-treatment, *Appl. Surf. Sci.* 426 (2017) 674-687.
- [56] P. Zhang, F.Y. Lv, A review of the recent advances in superhydrophobic surfaces and the emerging energy-related applications, *Energy*, 82 (2015) 1068-1087.
- [57] T.-L. Chen, J.-M. Ting, Correlation between seed layer characteristics and structures/properties of chemical bath synthesized ZnO nanowires, *Surf. Coat. Technol.* 303 (2016) 197-202.
- [58] J.-S. Park, I. Mahmud, H.J. Shin, M.-K. Park, A. Ranjesh, D.K. Lee, H.-R. Kim, Effect of surface energy and seed layer annealing temperature on ZnO seed layer formation and ZnO nanowire growth, *Appl. Surf. Sci.* 362 (2016) 132-139.
- [59] H. Li, C. Huang, L. Zhang, W. Lou, Fabrication of superhydrophobic surface on zinc substrate by 3-trifluoromethylbenzene diazonium tetrafluoroborate salts, *Appl. Surf. Sci.* 314 (2014) 906-909.
- [60] C. Chen, S. Yang, L. Liu, H. Xie, H. Liu, L. Zhu, X. Xu, A green one-step fabrication of superhydrophobic metallic surfaces of aluminum and zinc, *J. Alloy. Compd.* 711 (2017) 506-513.
- [61] Y. Qing, C. Yang, Q. Zhao, C. Hu, C. Liu, Simple fabrication of superhydrophobic/superoleophobic surfaces on copper substrate by two-step method, *J. Alloys Compd.* 695 (2017) 1878-1883.

- [62] W. Sun, L. Wang, Z. Yang, S. Li, T. Wu, G. Liu, Fabrication of polydimethylsiloxane-derived superhydrophobic surface on aluminium via chemical vapour deposition technique for corrosion protection, *Corros. Sci.* 128 (2017) 176-185.
- [63] T. Xiang, M. Zhang, C. Li, S. Zheng, S. Ding, J. Wang, C. Dong, L. Yang, A facile method for fabrication of superhydrophobic surface with controllable water adhesion and its applications, *J. Alloys Compd.* 704 (2017) 170-179.
- [64] D. Tian, X. Zhang, X. Wang, J. Zhai, L. Jiang, Micro/nanoscale hierarchical structured ZnO mesh film for separation of water and oil, *Phys. Chem. Chem. Phys.* 13 (2011) 14606-14610.
- [65] A.B.D. Cassie, S. Baxter, Wettability of porous surfaces, *Trans. Faraday Soc.* 40 (1944) 546-551.
- [66] H. Wang, C. Xie, Controlled fabrication of nanostructured ZnO particles and porous thin films via a modified chemical bath deposition method, *J. Cryst. Growth.* 291 (2006) 187-195.
- [67] Y. Chen, Z. Tong, L. Luo, Boron Nitride Nanowires Produced on Commercial Stainless Steel foil, *Chinese J. Chem. Eng.* 16 (2008) 485-487.
- [68] A.V. Rudakova, U.G. Oparicheva, A.E. Grishina, A.A. Murashkina, A.V. Emeline, D.W. Bahnemann, Photoinduced hydrophilic conversion of hydrated ZnO surfaces, *J. Colloid Interface Sci.* 466 (2016) 452-460.
- [69] R.-D. Sun, A. Nakajima, A. Fujishima, T. Watanabe, K. Hashimoto, Photoinduced Surface Wettability Conversion of ZnO and TiO₂ Thin Films, *J. Phys. Chem B.* 105 (2001) 1984-1990.
- [70] N. Asakuma, T. Fukui, M. Toki, K. Awazu, H. Imai, Photoinduced hydroxylation at ZnO surface, *Thin Solid Films*, 445 (2003) 284-287.
- [71] G. Qi, H. Zhang, Z. Yuan, Superhydrophobic brocades modified with aligned ZnO nanorods, *Appl. Surf. Sci.* 258 (2011) 662-667.
- [72] H. Hu, H.-F. Ji, Y. Sun, The effect of oxygen vacancies on water wettability of a ZnO surface, *Phys. Chem. Chem. Phys.* 15 (2013) 16557-16565.
- [73] I. Gromyko, M. Krunk, T. Dedova, A. Katerski, D. Klauson, I. Oja Acik, Surface properties of sprayed and electrodeposited ZnO rod layers, *Appl. Surf. Sci.* 405 (2017) 521-528.
- [74] P. Suresh Kumar, J. Sundaramurthy, D. Mangalaraj, D. Nataraj, D. Rajarathnam, M.P. Srinivasan, Enhanced super-hydrophobic and switching behavior of ZnO nanostructured surfaces prepared by simple solution – Immersion successive ionic layer adsorption and reaction process, *J. Colloid Interface Sci.* 363 (2011) 51-58.
- [75] J. Światowska-Mrowiecka, S. Zanna, K. Ogle, P. Marcus, Adsorption of 1,2-diaminoethane on ZnO thinfilms from p-xylene, *Appl. Surf. Sci.* 254 (2008) 5530-5539.
- [76] E. McCafferty, J.P. Wightman, Determination of the concentration of surface hydroxyl groups on metal oxide films by a quantitative XPS method, *Surf Interface Anal.* 26 (1998) 549-564.
- [77] D. Pradhan, K.T. Leung, Vertical Growth of Two-Dimensional Zinc Oxide Nanostructures on ITO-Coated Glass: Effects of Deposition Temperature and Deposition Time, *J. Phys. Chem. C*, 112 (2008) 1357-1364.
- [78] E. De la Rosa, S. Sepúlveda-Guzman, B. Reesha-Jayan, A. Torres, P. Salas, N. Elizondo, M.J. Yacamán, Controlling the Growth and Luminescence Properties of Well-Faceted ZnO Nanorods, *J. Phys. Chem. C*. 111 (2007) 8489-8495.
- [79] O. Lupan, T. Pauporté, L. Chow, B. Viana, F. Pellé, L.K. Ono, B. Roldan Cuenya, H. Heinrich, Effects of annealing on properties of ZnO thin films prepared by electrochemical deposition in chloride medium, *Appl. Surf. Sci.* 256 (2010) 1895-1907.
- [80] D.J. Qiu, H.Z. Wu, A.M. Feng, Y.F. Lao, N.B. Chen, T.N. Xu, Annealing effects on the microstructure and photoluminescence properties of Ni-doped ZnO films, *Appl. Surf. Sci.* 222 (2004) 263-268.
- [81] H. Liu, L. Feng, J. Zhai, L. Jiang, D. Zhu, Reversible Wettability of a Chemical Vapor Deposition Prepared ZnO Film between Superhydrophobicity and Superhydrophilicity, *Langmuir*, 20 (2004) 5659-5661.
- [82] M.T.Z. Myint, N.S. Kumar, G.L. Hornyak, J. Dutta, Hydrophobic/hydrophilic switching on zinc oxide micro-textured surface, *Appl. Surf. Sci.* 264 (2013) 344-348.
- [83] H. Luo, J. Ma, P. Wang, J. Bai, G. Jing, Two-step wetting transition on ZnO nanorod arrays, *Appl. Surf. Sci.* 347 (2015) 868-874.

- [84] R. Wang, K. Hashimoto, A. Fujishima, M. Chikuni, E. Kojima, A. Kitamura, M. Shimohigoshi, T. Watanabe, Light-induced amphiphilic surfaces, *Nature*, 388 (1997) 431-432.
- [85] F.M. Fowkes, Calculation of Work of Adhesion by Pair Potential Summation, in: F.M. Fowkes (Ed.) *Hydrophobic Surfaces*, Academic Press, 1969, pp. 151-163.
- [86] C. Mrabet, N. Mahdhi, A. Boukhachem, M. Amlouk, T. Manoubi, Effects of surface oxygen vacancies content on wettability of zinc oxide nanorods doped with lanthanum, *J. Alloys Compd.*, 688 (2016) 122-132.
- [87] J. Yong, F. Chen, Q. Yang, D. Zhang, U. Farooq, G. Du, X. Hou, Bioinspired underwater superoleophobic surface with ultralow oil-adhesion achieved by femtosecond laser microfabrication, *J. Mater. Chem. A*, 2 (2014) 8790-8795.
- [88] J. Lü, K. Huang, X. Chen, J. Zhu, F. Meng, X. Song, Z. Sun, Reversible wettability of nanostructured ZnO thin films by sol-gel method, *Appl. Surf. Sci.* 256 (2010) 4720-4723.
- [89] J. Lü, K. Huang, X. Chen, J. Zhu, F. Meng, X. Song, Z. Sun, Enhanced photo-induced hydrophilicity of the sol-gel-derived ZnO thin films by Na-doping, *Appl. Surf. Sci.* 257 (2011) 2086-2090.
- [90] M. Miyauchi, A. Nakajima, T. Watanabe, K. Hashimoto, Photocatalysis and Photoinduced Hydrophilicity of Various Metal Oxide Thin Films, *Chem. Mater.* 14 (2002) 2812-2816.
- [91] R. Parize, J. Garnier, O. Chaix-Pluchery, C. Verrier, E. Appert, V. Consonni, Effects of Hexamethylenetetramine on the Nucleation and Radial Growth of ZnO Nanowires by Chemical Bath Deposition, *J. Phys. Chem. C*, 120 (2016) 5242-5250.
- [92] S.B. Yahia, L. Znaidi, A. Kanaev, J.P. Petit, Raman study of oriented ZnO thin films deposited by sol-gel method, *Spectrochim. Acta A. Mol. Biomol. Spectrosc.* 71 (2008) 1234-1238.
- [93] K. Yadav, B.R. Mehta, S. Bhattacharya, J.P. Singh, A fast and effective approach for reversible wetting-dewetting transitions on ZnO nanowires, *Nature*, 6 (2016) 35073.
- [94] Q. Li, F. Tang, C. Wang, X. Wang, Facile fabrication of wear-resistant multifunctional surfaces on titanium alloy substrate by one-step anodization and modification with silicon dioxide nanoparticles, *J. Sol-Gel Sci. Technol.* 80 (2016) 318-325.
- [95] S. Adam, K.N. Barada, D. Alexander, C.G. Mool, L. Eric, Linear abrasion of a titanium superhydrophobic surface prepared by ultrafast laser microtexturing, *J. Micromech. Microeng.* 23 (2013) 115012-115020.
- [96] A. Steele, I. Bayer, E. Loth, Adhesion strength and superhydrophobicity of polyurethane/organoclay nanocomposite coatings, *J. Appl. Polym. Sci.* 125 (2012) E445-E452.
- [97] L. Wu, J. Zhang, B. Li, L. Fan, L. Li, A. Wang, Facile preparation of super durable superhydrophobic materials, *J. Colloid Interface Sci.* 432 (2014) 31-42.
- [98] S.S. Lathe, P. Sudhagar, A. Devadoss, A.M. Kumar, S. Liu, C. Terashima, K. Nakata, A. Fujishima, A mechanically bendable superhydrophobic steel surface with self-cleaning and corrosion-resistant properties, *J. Mater. Chem A*, 3 (2015) 14263-14271.
- [99] F. Su, K. Yao, Facile Fabrication of Superhydrophobic Surface with Excellent Mechanical Abrasion and Corrosion Resistance on Copper Substrate by a Novel Method, *ACS Appl. Mater. Interfaces*, 6 (2014) 8762-8770.
- [100] L. Liu, F. Xu, L. Ma, Facile Fabrication of a Superhydrophobic Cu Surface via a Selective Etching of High-Energy Facets, *J. Phys. Chem C*, 116 (2012) 18722-18727.
- [101] X. Yonghao, L. Yan, W.H. Dennis, C.P. Wong, Mechanically robust superhydrophobicity on hierarchically structured Si surfaces, *Nanotechnol.* 21 (2010) 155705.

List of figure captions

Fig. 1 Optical image of water and hexane droplets: (a) on the as-prepared ZnO surface, (b) after annealing at 400 °C.

Fig. 2 Changes of WCA and underwater OCA values vs. annealing cycles.

Fig. 3 Changes of water CAH and underwater oil CAH values vs. annealing cycles.

Fig. 4 SEM images of the 304-stainless-steel mesh surface :(a) bare substrate, (b) with seed layer of ZnO, (c) and (d) as- prepared ZnO surface, (e) and (f) after annealing at 400° C.

Fig. 5 XRD pattern of samples: (a) as-prepared, (b) annealed sample at 400° C.

Fig. 6 XPS wide survey spectra of samples: (a) as-prepared, (b) annealed at 400° C.

Fig. 7 XPS O 1s spectra of samples: (a) as-prepared, (b) annealed at 400° C.

Fig. 8 Raman spectra of samples: (a) as-prepared, (b) After annealing at 400°C, (C) After annealing at 150° C.

Fig. 9 Variations in WCA values related to the as-prepared superhydrophobic sample after abrasion cycles.

Fig.10 SEM images of superhydrophobic surface after abrasion of 20 cycles. (a) low magnification and (b) high magnification.

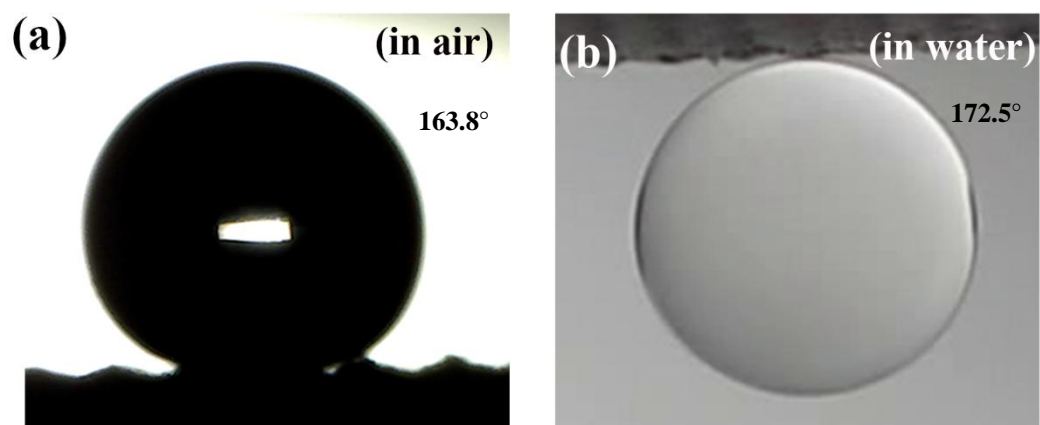


Fig.1 Optical image of water and hexane droplets: (a) on the as-prepared ZnO surface, (b) after annealing at 400 °C.

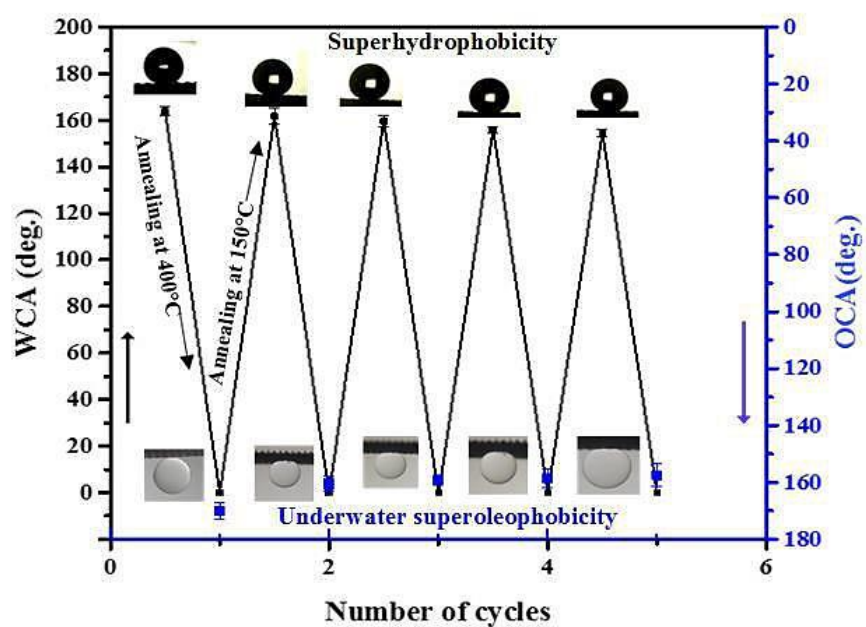


Fig. 2 Changes of WCA and underwater OCA values vs. annealing cycles.

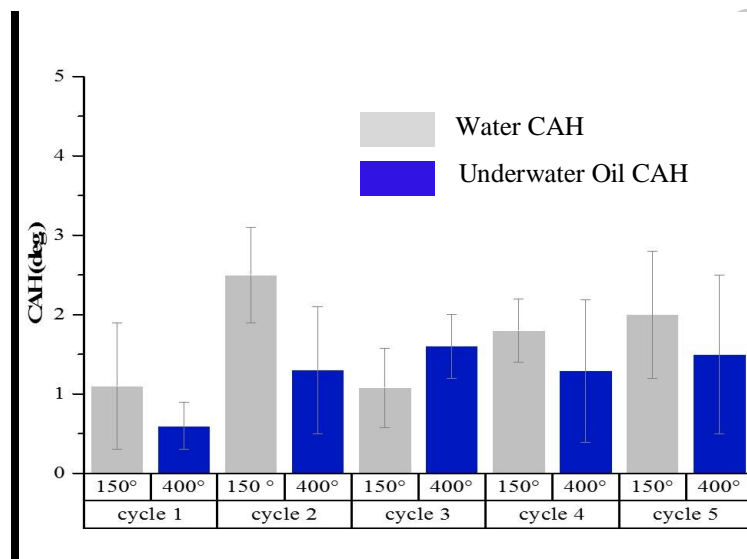


Fig.3 Water droplet and underwater oil droplet CAH values vs. annealing cycles.

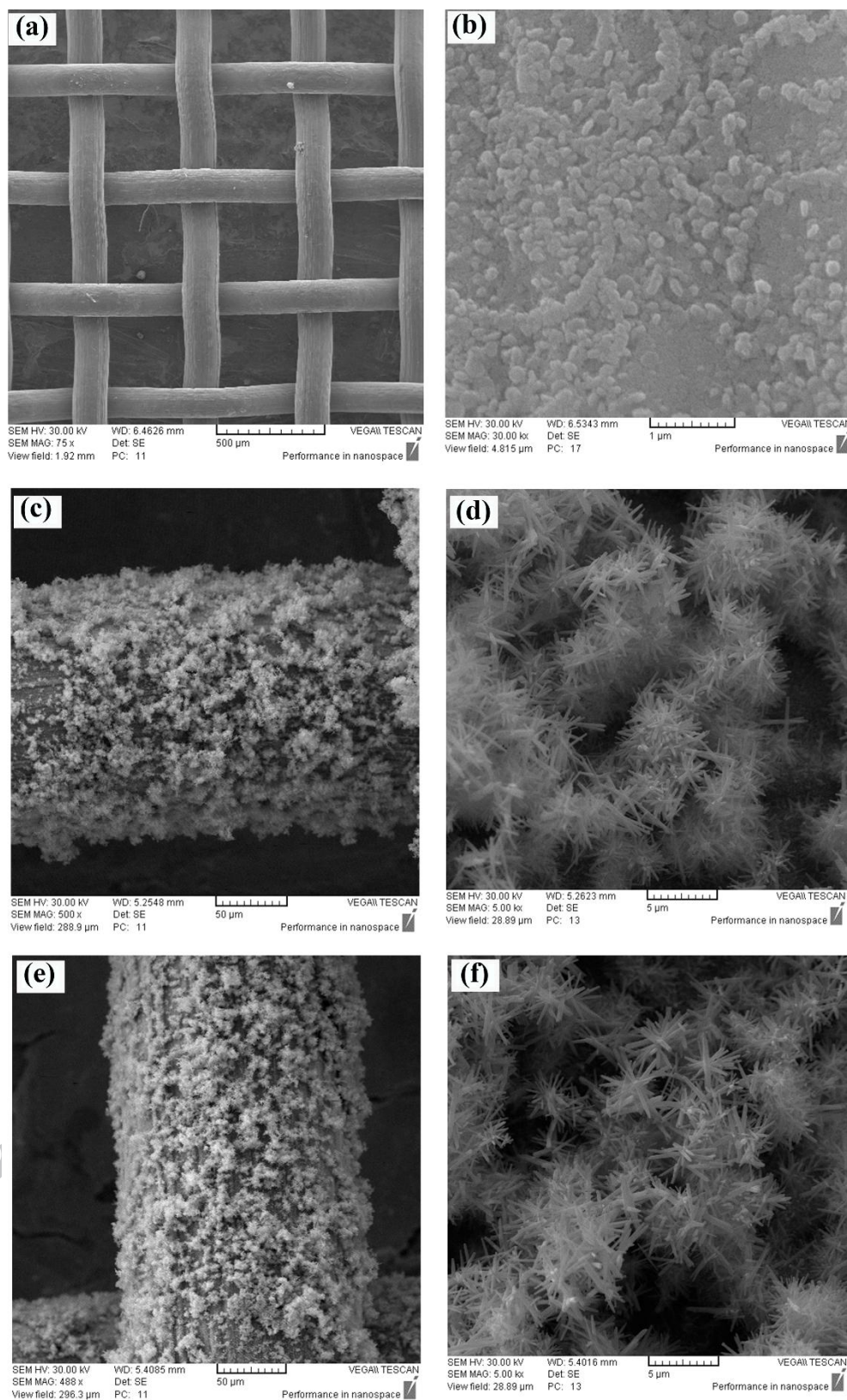


Fig.4 SEM images of the 304-stainless-steel mesh surface :(a) bare substrate, (b) with seed layer of ZnO, (c) and (d) as- prepared ZnO surface, (e) and (f) after annealing at 400° C.

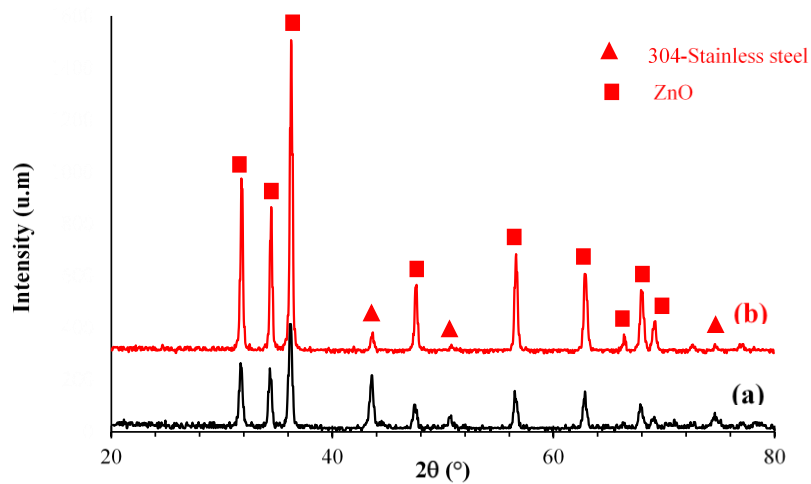


Fig.5 XRD pattern of samples: (a) as-prepared, (b) annealed sample at 400° C.

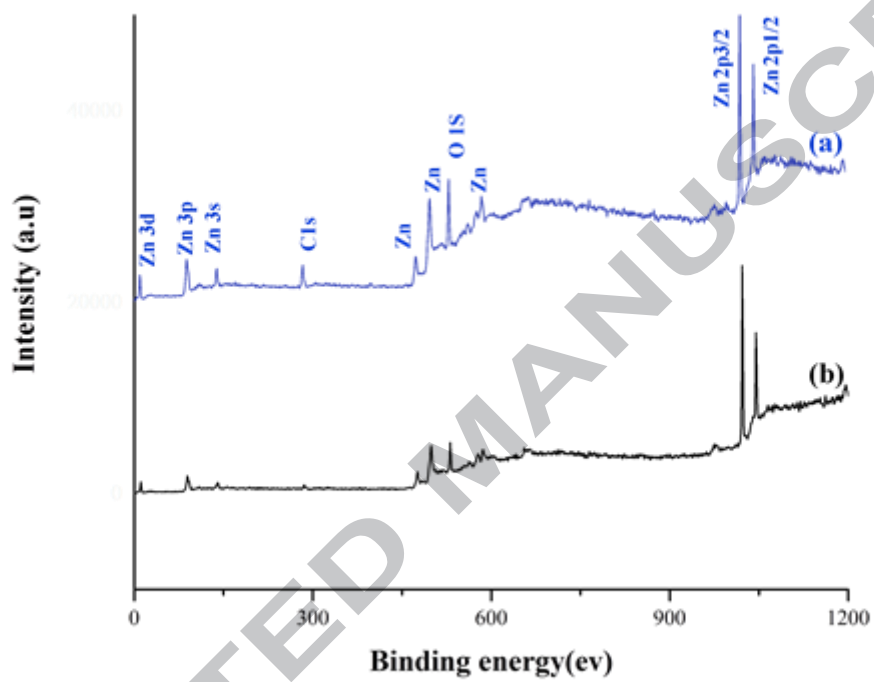


Fig. 6 XPS wide survey spectra of samples: (a) as-prepared, (b) annealed at 400° C

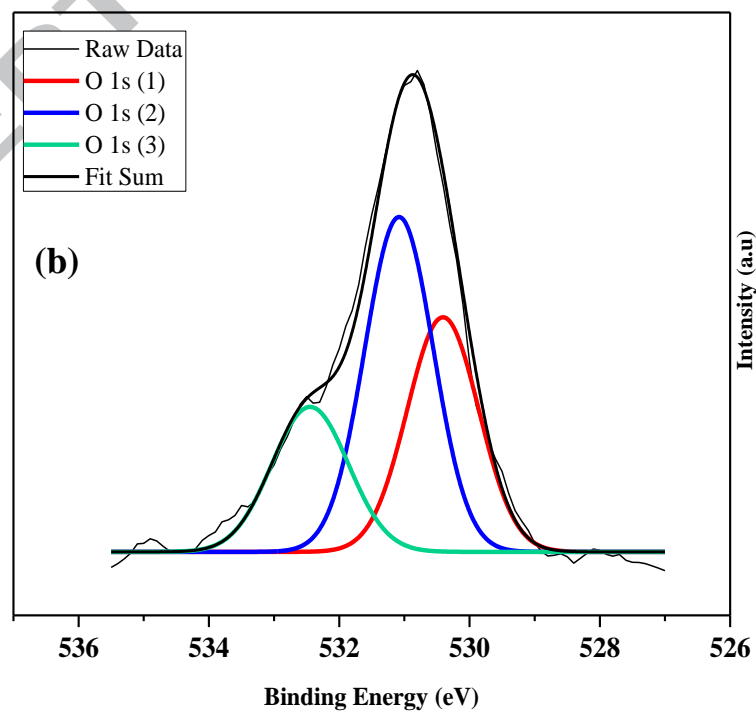
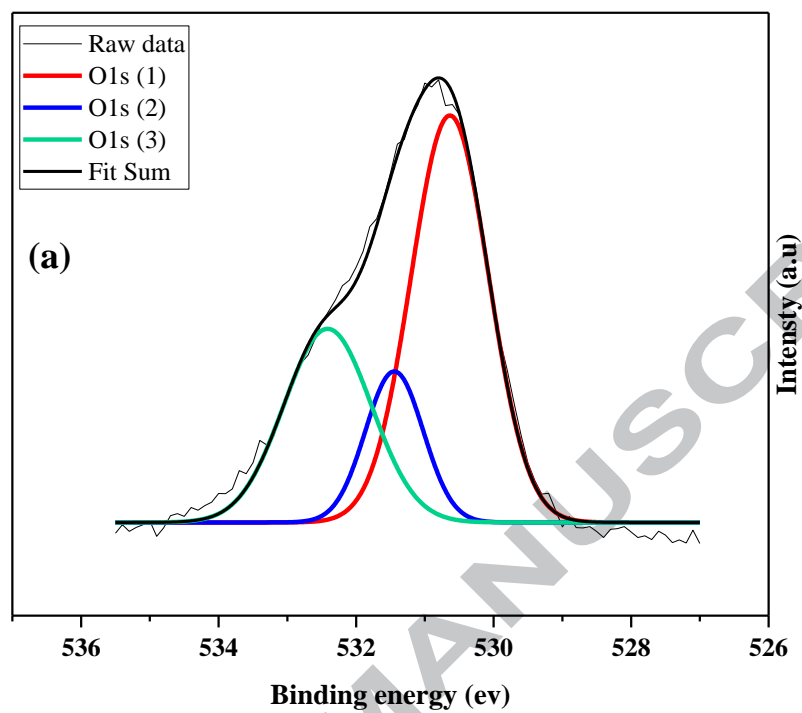


Fig. 7 XPS O 1s spectra of samples: (a) as-prepared, (b) annealed at 400° C.

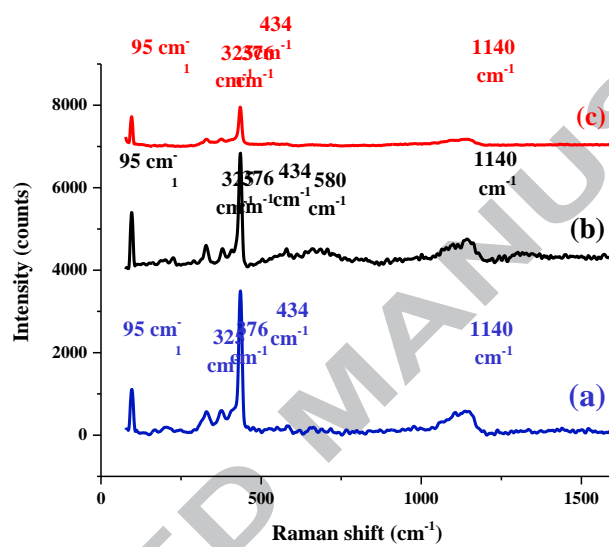


Fig. 8 Raman spectra of samples: (a) as-prepared, (b) After annealing at 400°C, (C) After annealing at 150° C.

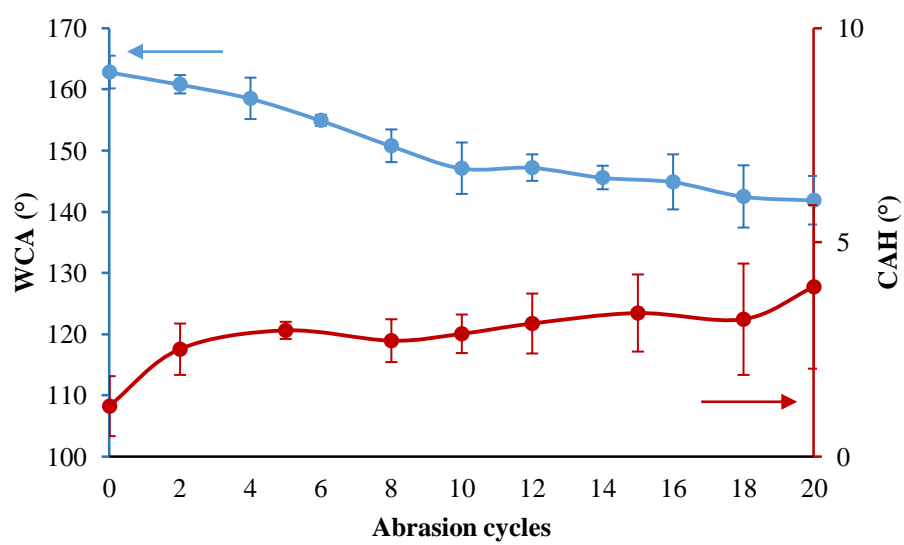


Fig.9 Variations in WCA values related to the as-prepared superhydrophobic sample after abrasion cycles.

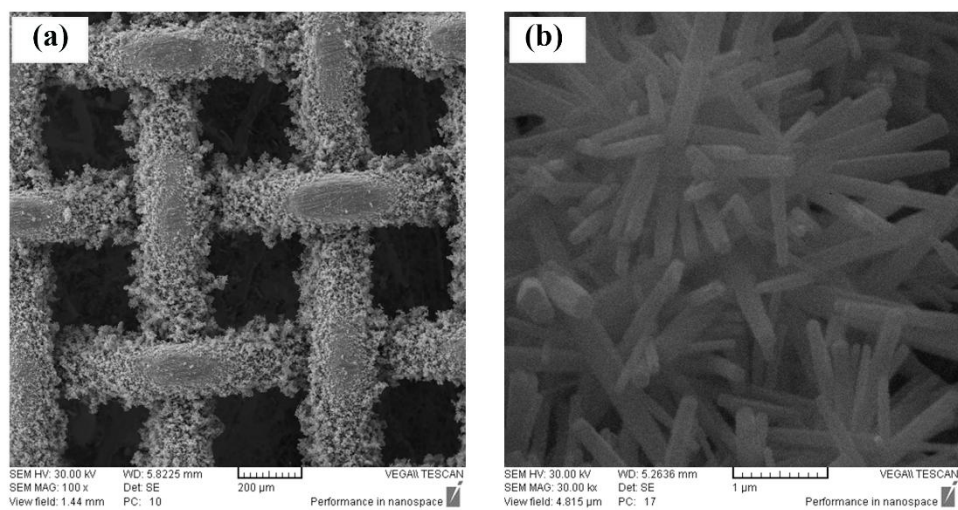


Fig.10 SEM images of superhydrophobic surface after abrasion of 20 cycles. (a) low magnification and (b) high magnification.

Research highlights

- Micro/nano structured superhydrophobic ZnO surface was prepared via a facile chemical bath deposition method.
- The prepared film exhibits superhydrophobic characteristics in air with a WCA of $163.8^\circ \pm 1.8^\circ$ and CAH of $1.1^\circ \pm 0.8^\circ$ applying no chemical post modification step.
- ZnO surface was switched to highly hydrophilic and underwater superoleophobic properties with an oil contact angle (OCA) of about 172.5° after being annealed at 400°C in air for 30 min
- ZnO surface can reversibly switch its wettability between superhydrophobicity and underwater oleophobicity just by varying the annealing temperature during a short time.
- The superhydrophobic surface possesses an excellent robustness after 20 abrasion cycles under the pressure of 4.7 KPa.